The International Journal of Advanced Manufacturing Technology (2023) 127:635–648
https://doi.org/10.1007/s00170-023-11562-3

ORIGINAL ARTICLE

Speed and torque control of pneumatic motors using controlled pulsating flow

Mohamed A. Aziz[1] · Ernesto Benini[2] · Mostafa E. A. Elsayed[3] · Mohamed A. Khalifa[4] · Osama A. Gaheen[4]

Received: 15 November 2022 / Accepted: 5 May 2023 / Published online: 16 May 2023

Abstract

Pneumatic motors have several advantages and have many robotics and automation applications. The importance of the study is that it is a cheap and possible way to apply it to the fixed displacement pneumatic motors with simple directional control valve used. The purpose of the addition to any traditional pneumatic motors is to change the fixed displacement pneumatic motor to be variable speed and torque compared to the expensive systems such as the proportional control valve in many industrial applications. The study also included validated simulations using the Automation Studio program to control the pneumatic motor's speed and torque. In addition, the results showed remarkable success in controlling the pneumatic motor outputs depending on the frequency of the compressed air-source pulses and pressure. The pulsating air frequencies of 1.5, 3, and 4.5 Hz were considered at different inlet source pressure changes from 1.72, 3.45, and 5.17 bar. As the pulsating flow frequency of compressed air decreased from 4.5, 3, and 1.5 Hz, the motor pressure and torque decreased. Furthermore, empirical correlations related to frequency and pressure effect have been developed. The error is 6.3–9.5% in predicting the motor speed and torque outputs. The limitation of the proposed method in real-life applications is about a maximum of 7.5 bar. On the other hand, the frequency is limited to 9 Hz using a mechanical solenoid.

Keywords Pneumatic motor · Pneumatic actuator control · Output performance · High-speed directional control valve · Pulsating flow · Speed control · Torque control

Nomenclature

A	Inner cylinder area (m^2)
a	Piston rod area (m^2)
D	Inner cylinder diameter (m)
d	Cylinder rod diameter (m)
f	Frequency (Hz)
P	Pressure (bar)
Q	Flow rate (L/s)
q	Motor displacement per revolution (cm^3/rev)
F	Force (N)
L	Cylinder length (m)
N	Motor revolution speed (rpm)
T	Torque (Nm)
V	Cylinder velocity (m/s)
$\dot{W}$	Power (w)
η_m	Mechanical efficiency
η_v	Volumetric efficiency

Subscripts

act	Actual
th	Theoritical
e	Exit
i	Inlet
r	Return
m	Motor
1	Piston side
2	Rod side

✉ Ernesto Benini
ernesto.benini@unipd.it

Mohamed A. Aziz
Mohamed.aziz@suezuni.edu.eg

Mostafa E. A. Elsayed
mustafa.elsayed@feng.bu.edu.eg

Mohamed A. Khalifa
eng_mkhalifa@yahoo.com

Osama A. Gaheen
osama_gaheen@yahoo.com; Osama.Gaheen@iaet.edu.eg

[1] College of Engineering, Suez University, Suez, Egypt

[2] Dipartimento Di Ingegneria Industriale, Università Degli Studi Di Padova, Via Venezia 1, 35131 Padua, Italy

[3] Automation and Energy Technology Lab, Mechanical Engineering Department, Shoubra Faculty of Engineering, Benha University, Cairo, Egypt

[4] Institute of Aviation Engineering and Technology, Giza, Egypt

1 Introduction

Electric motors are widely used in robotics and automation applications because of their precise control, low maintenance, cleanliness, and ease of operation. However, they have many drawbacks, such as being large in size and heavy in weight. On the other hand, pneumatic motors have a high power-to-weight ratio, high speed, and various ways to transmit power based on a simple operational mechanism using compressed air. Nevertheless, for a long period, simple control mechanisms have used pneumatic actuators in industrial applications. This is because pneumatic motors' high-precision and rapid control are complex and expensive. This is due to a high-order time-varying actuator dynamics, air compressibility effect, and other factors such as static friction, with a wide range of differences in payload and pressure.

Two approaches are usually used to improve pneumatic actuator control performance. The first takes the software approach, which includes advanced modern technologies such as model-based control, adaptive control, sliding, and position control. The approach maximizes the control performance of pneumatic actuators' outputs [1–5]. The second approach enhances hardware to optimize pneumatic actuators. It is characterized by a strong endurance of friction factors and other changes in system parameters over time [6]. Some researchers [7, 8] used a PID controller in a built-in control system integrated with feedback linearization, which acts as an intermediate pressure control loop to cancel the nonlinearity arising from air usage. Renn et al. [9] combined a linear PID controller and a nonlinear fuzzy sliding-mode controller to control the RPM of a servo-pneumatic motor. The results showed the possibility of developing pneumatic actuators with the proposed control system.

Chen et al. [10] proposed a specially designed pneumatic motor for a powerful and precise operation, combined with a gearbox to provide a range of variable gear ratio options. The motor can adapt to different operating requirements. Their application resulted in a pneumatic motor similar to conventional electric motors and offered more flexibility in an MR-conditional robot design. Early development of pneumatic/electric hybrid actuators can be found in the literature. A system in which a small electric motor is coupled to a pneumatic actuator. This results in more efficient hybrid actuators in damping and easier control than conventional pneumatic actuators [11–13]. Stoianovici et al. [14] introduced a new type of pneumatic motor, a pneumatic stepper motor. The study clarified the availability of the pneumatic step proposed for other pneumatic or hydraulic precision-motion applications.

Chen et al. [15] presented an adaptive speed control system for a vane-type pneumatic motor controlled using an electronic throttle. The results showed the accuracy and robustness of the adaptive dynamic sliding-mode control system for nonlinear and time-varying pneumatic servo systems. Recently, researchers have been attracted to pneumatic motor applications in many engineering fields such as transportation [16] and energy storage devices [17]. The state of art related to current research ideas in literature includes synchronous motors [18], clutch sleeve and shell [19, 20], and pipeline elbow [20, 21].

Studies on hardware enhancement for pneumatic motors are relatively few despite the many advantages offered in their trending applications in transportation and industry. However, the performance control of pneumatic motors is not satisfactory mainly due to air compressibility and the high cost of conventional control methods using proportional control valves. This paper presents an unprecedented application of pneumatic motor control using a pulsating compressed air technique. Therefore, this research focused on a simple, innovative method, cheap and easy to install on pneumatic motor systems. The application idea focuses on controlling the pneumatic motor outputs, such as rotational speed and torque, using a pulse flow of compressed air. It can be controlled by a source pressure and pulse frequency.

The paper is organized as follows. Section 2 describes the pneumatic motor system, including its governing equation, electro-pneumatic motor circuit, and pulse generation through frequency change with the PLC method using Automation Studio simulation software. Section 3 demonstrates the application of the software to simulate the pneumatic motor and validation with experimental results of a pneumatic cylinder. Section 4 discusses the influence of pulsating flow at source pressures of 1.72, 3.45, and 5.17 bar and frequencies of 1.5, 3, and 4.5 Hz. Next, a mathematical correlation is generated to predict a more applicable range of applications through the collected output data in Sect. 5. Finally, Sect. 6 provides conclusions for the present work.

2 Description of the pneumatic system

2.1 Governing equations of pneumatic motor

To obtain deeper insights into the output mechanical energy of the actuator, a simplified model is developed. The model considered the main governing equations for a pneumatic motor. The torque and rotational speed depend on the pneumatic motor's air inlet pressure and flow rate. The fixed-displacement unidirectional pneumatic motor is shown in Fig. 1.

The theoretical and actual motor torques are calculated from:

$$T_{theo} = \frac{q_m P_m}{2\pi} \tag{1}$$

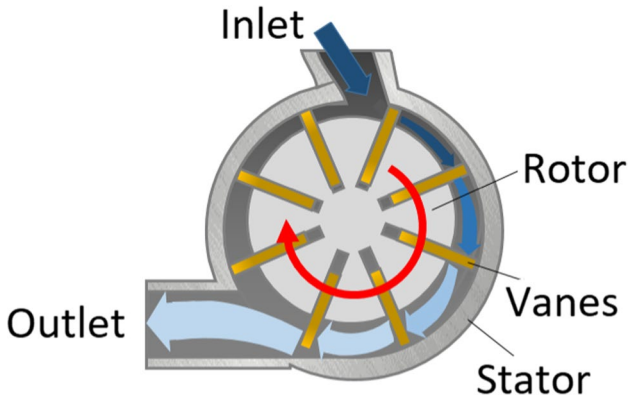

Fig. 1 Fixed-displacement unidirectional pneumatic motor

$$T_{act} = \frac{q_m P_m}{2\pi}\eta_m \tag{2}$$

In addition, the output theoretical motor power is calculated from

$$\dot{W}_{theo} = T_{theo}.\, N = \frac{q_m P_m N}{2\pi} \tag{3}$$

Moreover, the theoretical and actual motor flow rates are calculated from

$$Q_{theo} = q_m N \tag{4}$$

$$Q_{actual} = q_m N \eta_v \tag{5}$$

From the previous equations, the pneumatic motor performance depends on q_m and P_m.

2.2 Electro-pneumatic motor circuit

Any pneumatic and hydraulic system is constructed mainly from three main stages. It begins with converting mechanical energy input to fluid power with hydraulic pumps or air compressors. Then, the fluid power is transmitted through pipes and connectors while its direction, pressure, and flow rate are controlled through a control element. Finally, the fluid power is converted into mechanical power by actuators such as cylinders and motors. The pneumatic circuit diagram for a pneumatic motor is shown in Fig. 2. It consists of a pressurized air source, adjustable relief valve, 5/3 direction control valve solenoids operated normally in closed mode, pressure gauges, and fixed-displacement unidirectional pneumatic motor. Pulsating flow technique was used in controlling the amount of fluid flow per second according to the frequency at inlet pressures of 1.72, 3.45, and 5.17 bar. The pulsating flow was generated at 1.5, 3, and 4.5 Hz frequencies. On the other hand, the required frequency changes through an electric control circuit designed particularly for this purpose.

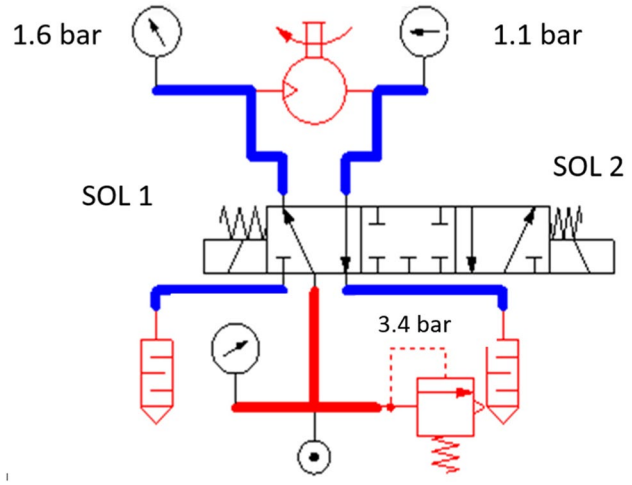

Fig. 2 Pneumatic circuit diagram for a fixed-displacement unidirectional pneumatic motor

2.3 Automation Studio simulation setup

Automation Studio is used for training purposes. It can be applied in designing, training, and troubleshooting simulations of hydraulics, pneumatics, and electrical control systems [22]. The Automation Studio is a completely integrated software package. It contains a comprehensive library used to design, simulate, and animate electro-pneumatic circuits with interface availability for ladder and electric control circuits. The motor torque and speed controls were simulated with the program using pulsating flow at different pressures (1.72, 3.45, and 5.17 bar) and frequencies (1.5, 3, and 4.5 Hz). The simulated electro-pneumatic circuits matched the actual system setup. A pulse flow can be created through the electrical control circuit that opens and closes the solenoids at a specific rate. It can be changed in the program according to the input frequency. Figure 3 shows the PLC control circuit. The momentary cyclic signal of the directional control solenoid valve is in the PLC output module. The interface between the pneumatic and control circuits was created with the Automation Studio program. The PLC control circuit was used at a frequency range greater than that of the classic control circuit.

3 Validation of automation studio simulation

To validate the Automation Studio results, an experimental system setup was built. The system was designed to measure the speed and force of the cylinder rod by applying continuous and controlled pulsating flow frequency

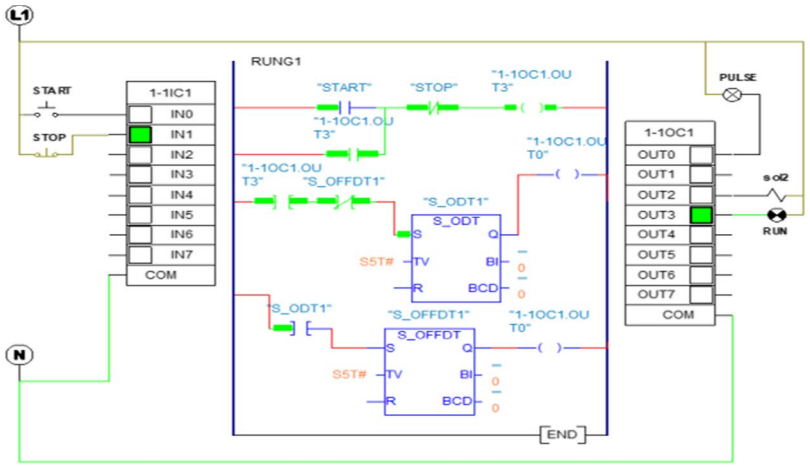

Input module Ladder Program Output module

(A)

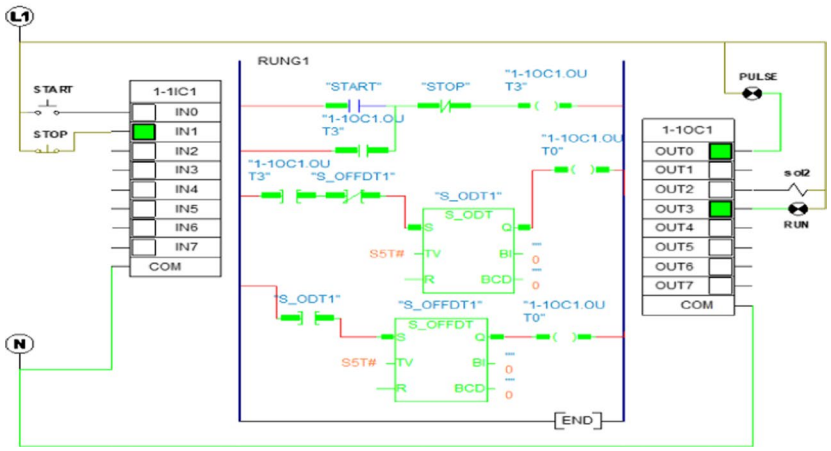

Input module Ladder Program Output module

(B)

Fig. 3 A schematic of the PLC control circuit. **A** Activate pulse generator. **B** De-activate pulse generator

at pressures 1.72, 3.45, and 5.17 bar. It was validated at 5.17 bar, a pressure used in real pneumatic system applications. The pulsating flow was generated at 3 Hz. The experimental system consists of a double-acting pneumatic cylinder, 3/5 directional control valve solenoid operated with high-speed solenoid, air compressor, pressure regulator, easy scope, pulse generation circuit with classic control circuit [23], meter data logger for airflow, and air pressure data logger. Figure 4A–C shows the experimental system setup.

Figure 5 compares simulation results and experimental measurements for the working pressure of the cylinder at continuous and pulsating flows of 3 Hz. The simulations were conducted using the Automation Studio program at similar experimental conditions and an input source pressure of 5.17 bar. An excellent agreement with the experimental data was obtained regarding trends. Figure 5 A and B show that the maximum pressure value inside the cylinder simulated by the Automation Studio program was below 2.8% and 1.1% for continuous and pulsating cases, respectively, compared with experimental measurements. The main pressure dropped from 5 to 2.12 bar by changing the operation mode from continuous to the pulsating flow of 3 Hz. This indicates that the pulse flow can affect the cylinder forces. On the other side, the simulation with the Automation Studio was a successful method for predicting the cylinder pressure at any frequency.

Figure 6A and B compare the simulation results and experimental measurements of the non-dimensional air volume as a percentage of the pneumatic cylinder volume as an indication of piston rod velocity. From the experimental observations, the piston rod reached the full stroke

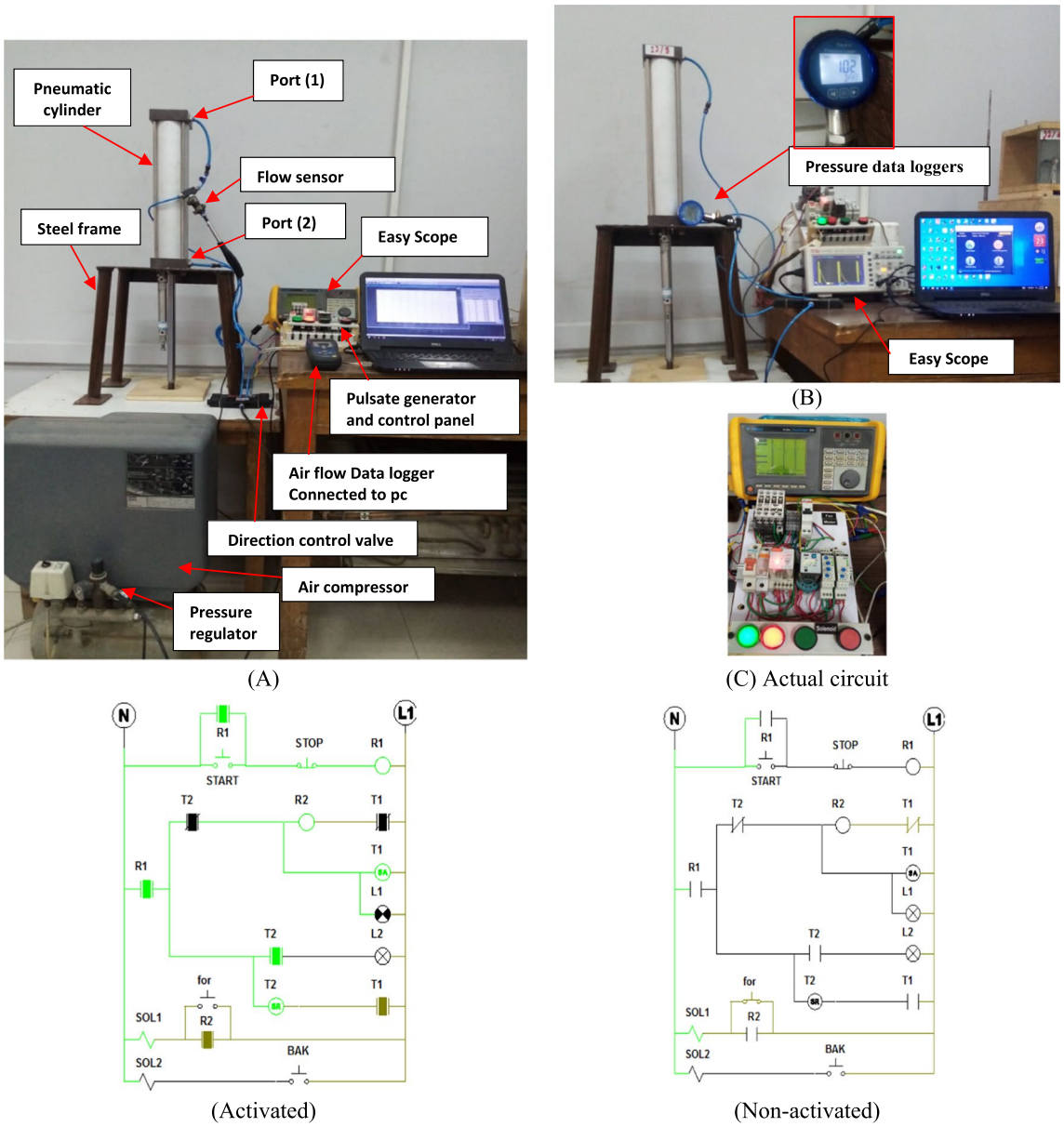

Fig. 4 Experimental system setups. **A** Air flow rate measurement at the cylinder, inlet **B** cylinder pressure measurement, **C** and **D** classic control circuit

(extreme position) at 80% of the non-dimensional air volume inside the cylinder. This is the air compressibility effect inside the cylinder and pressure accumulation. In the case of continuous flow, the time of the fully filled cylinder was 4 s by simulation, while from the experimental measurement, it filled 81.1% in 4 s. At a frequency of 3 Hz, the time of the fully filled cylinder was 18 s by simulation, while from the experimental measurement, it filled 81.6% at the same time. The increase in filling time from continuous mode to 3 Hz mode indicates the speed control. Figure 7A and B show the changes in flow rate with time inside the cylinder for experimental measurements and simulation results. A close agreement with the experimental data was achieved regarding trends.

The difference between the simulation results and experimental measurements for the continuous and pulse flow cases is related to the Automation Studio. The software does not take into account:

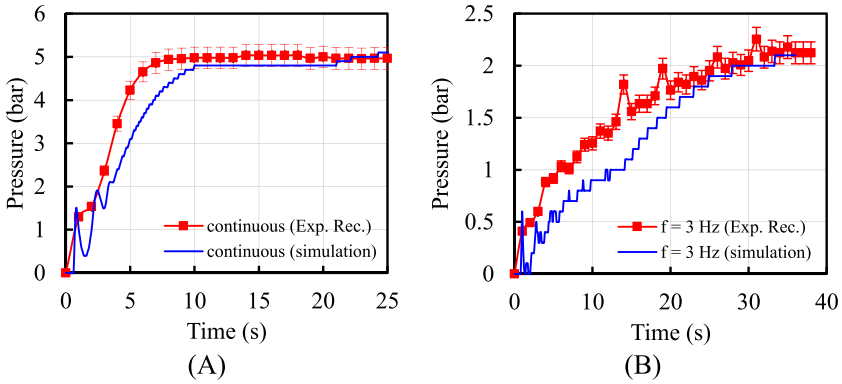

Fig. 5 Validation of pulsating effect on cylinder pressure: **A** continuous and **B** pulsate with a frequency of 3 Hz

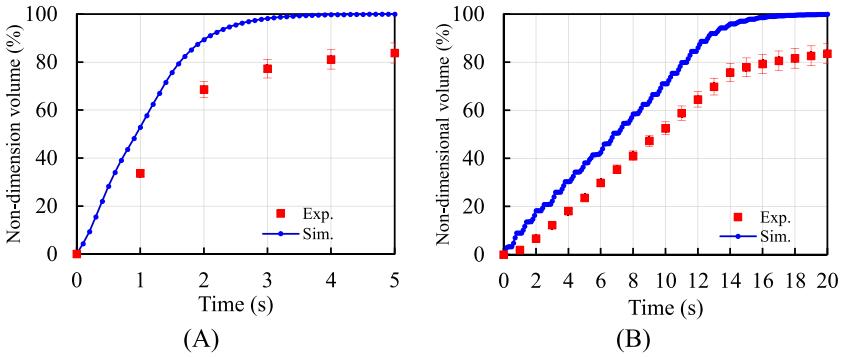

Fig. 6 Validation of pulsating effect on the percentage of non-dimensional air volume inside the cylinder: **A** continuous and **B** pulsate with a frequency of 3 Hz

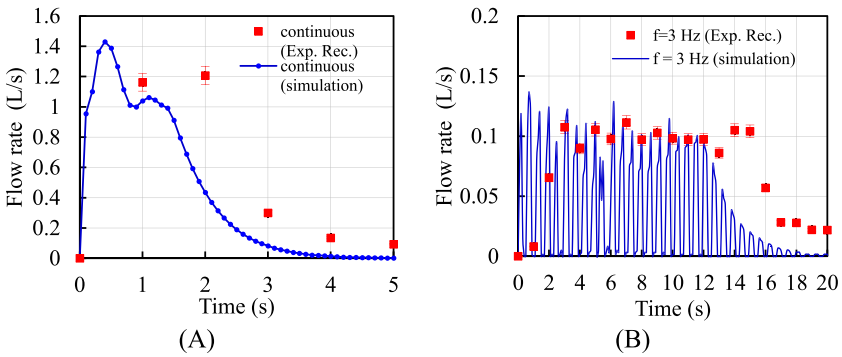

Fig. 7 Validation of pulsating effect on air flow rate inside the cylinder: **A** continuous and **B** pulsate with a frequency of 3 Hz

(1) The internal leakage inside the cylinder
(2) The internal leakage in the directional control valve
(3) The friction between the piston and cylinder
(4) Pressure loss in pipe fitting

In a real application, friction and leakage inside the cylinder and directional control valve cannot be neglected. In addition, the limited size (small) of the pressurized air tank affects invariable supply pressure in the experimental work. Besides the previously mentioned reasons for the difference between the simulation results and experimental measurements, the frequency in the experimental work was adjusted manually to the required frequencies. The adjustment was carried out through a control panel connected with an easy-scope device to count the number of pulses per second, leading to a certain resolution error in frequency change. The error can be handled using a PLC technique instead of the current classic control technique, which can minimize the frequency resolution error and give a variety of frequency range.

The Automation Studio simulated the difference between the continuous and pulsating flows with a maximum error of 2.8% compared with experimental measurements. The error margin is acceptable for evaluation and validation purposes. Hence, it is a good tool for simulating pulse flow inside pneumatic actuators with a robust and precise method. Furthermore, it is cheap and provides the view of actuator behavior at different modes of pulse frequencies without rebuilding a new setup.

4 Results and discussions

The influence of pulsating flow was studied with the Automation Studio program at main source pressures of 1.72, 3.45, and 5.17 bar and frequencies of 1.5, 3, and 4.5 Hz.

4.1 Pulsating flow at main source pressure, $P = 1.72$ bar

From Fig. 8, the average motor pressure decreases from 1.57 bar to 1.21, 1.35, and 1.53 bar by changing the flow mode from continuous flow to pulsating air flow of frequencies 1.5, 3, and 4.5 Hz, respectively. The motor torque directly depends on the inlet motor pressure, Eq. (2), so the input pressure is an important parameter controlling the motor torque.

The frequency change of the pulsating compressed air flow directly affects the motor speed, causing a noticeable drop. The drop in the motor speed increases as the frequency decreases, as shown in Fig. 9. The average motor speeds are 205, 99.4, 148.8, and 189 r.p.m at continuous flow mode, $f = 1.5$, 3, and 4.5 Hz, respectively. In addition, the fluctuations in motor speed r.p.m decrease with an increase in frequency and disappear at continuous flow. The fluctuations appeared because the motor was unloaded. On the other hand, the fluctuations decrease with the motor load increase, and the average stays at the same value.

It is worth noting the change in the internal pressure amplitude and rotational speed of the motor at different frequencies. For example, the amplitude changes from 1.31 to 0.72 to 0.30 bar at 1.5, 3, and 4.5 Hz. This behavior was also observed in the amplitude, which represents the motor rotational speed fluctuations.

Increasing the source pressure increases the air flow rate. As the source pressure increases, the loss rate inside the motor also increases due to the clearances inside the motor. Increasing the flow rate from the source overcomes the increase in the flow rate loss inside the motor. Therefore, the pressure gradient inside the motor increases with the pressure source, increasing the motor torque. A different mode of continuous and pulsating flows at frequencies 1.5, 3, and 4.5 Hz is shown in Figs. 8 and 9. As the pulsating flow frequency increases from 1.5 to 4.5 Hz, the percentages of average input pressure and motor r.p.m increase. The average input pressure decreased from 1.56 bar for the continuous mode to 1.53, 1.35, and 1.21 bar at 4.5, 3, and 1.5 Hz pulse flow frequencies. On the other hand, the same behavior is observed for the motor speed, where the average motor r.p.m decreased from

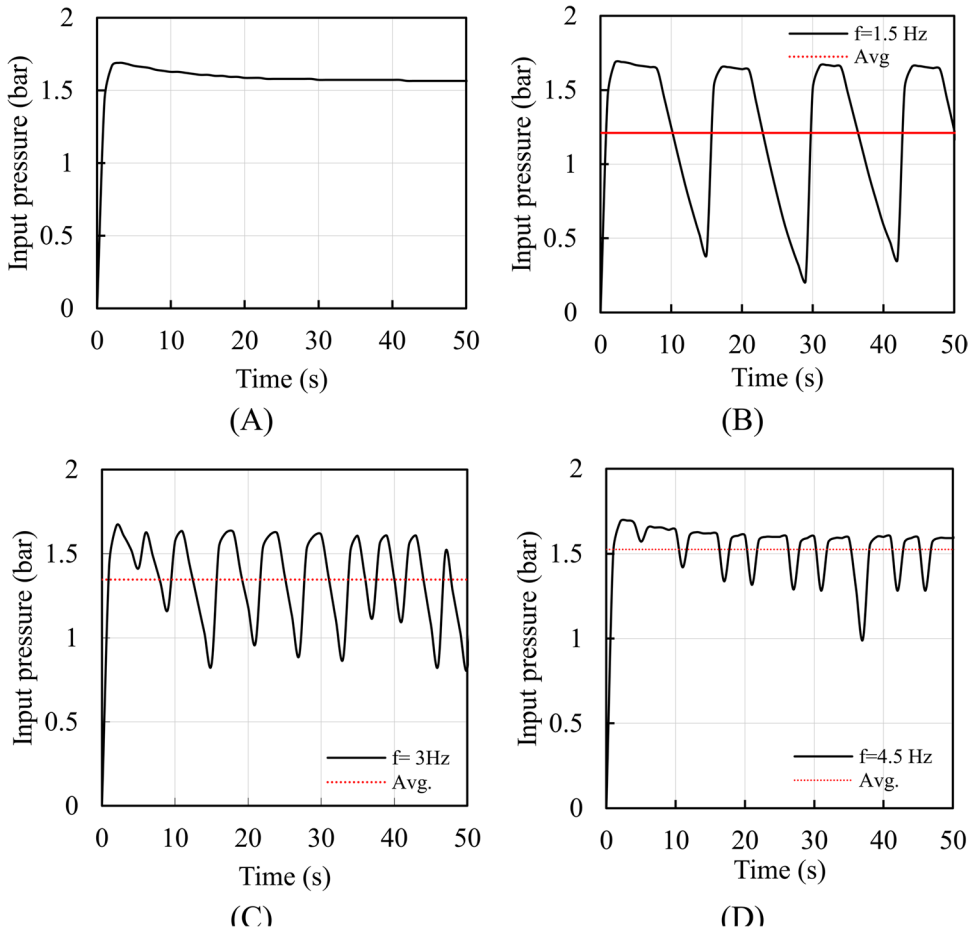

Fig. 8 Pneumatic motor pressure: **A** continuous, **B** $f = 1.5$ Hz, **C** $f = 3$ Hz, and **D** $f = 4.5$ Hz at main source pressure, $P = 1.72$ bar

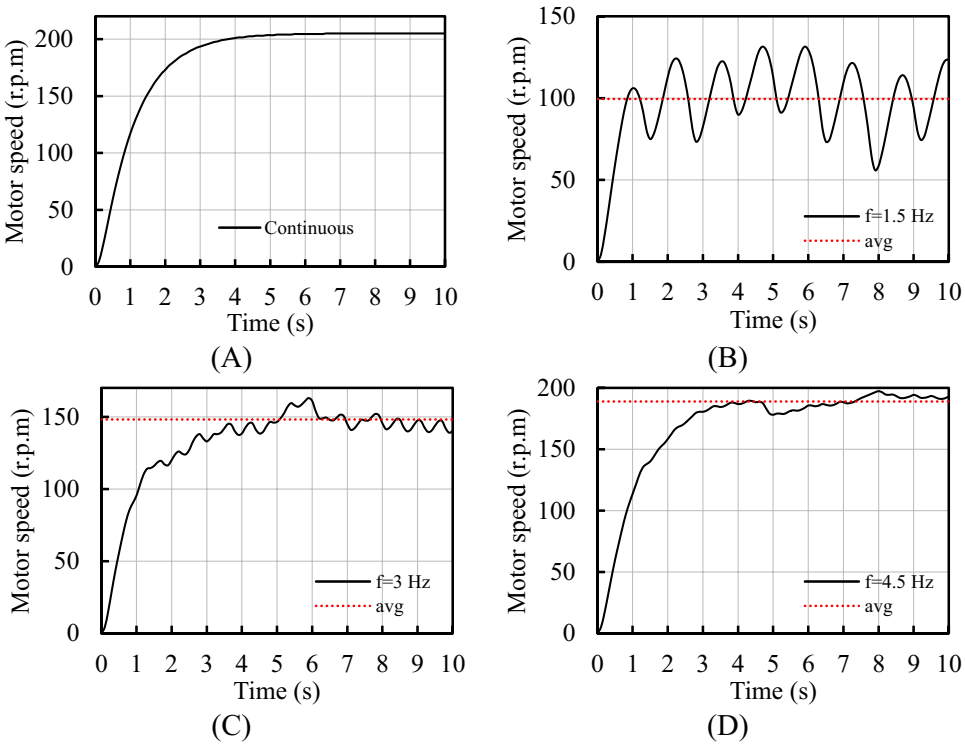

Fig. 9 Motor speed versus time at **A** continuous, **B** $f=1.5$ Hz, **C** $f=3$ Hz, and **D** $f=4.5$ Hz at main source pressure, $P=1.72$ bar

205 r.p.m for the continuous mode to 189.03, 148.18, and 99.43 r.p.m at 4.5, 3, and 1.5 Hz pulsating flow frequencies.

This gives a strong impression that pulsating flow influences the control of motor torque and r.p.m in the control of motor performance using different modes (pulse flow). It is worth mentioning and explaining the important factors affecting the simulation of the tensor performance and accuracy of the program outputs' results, such as compressibility, turbulence, and losses inside the pneumatic system (tubes, valves, motor, etc.). On the other hand, the effect of compression appears once with a constant value of the flow rate at a constant main pressure source. However, in the case of pulse flow, the fluid volume inside the motor undergoes repeated pressure and relaxation at each pulse. This volume changes as the motor rotates with the frequency. Therefore, the compressibility rate varies with the volume. In addition, with each repetitive pulse, the internal pressure of the charge inside the motor is affected by the pulse frequency, but in the case of a continuous flow, this effect appears only once at the beginning of the main pressure supplied by the source. This explains the motor's internal pressure change with the change in the pulse frequency.

4.2 Pulsating flow at main source pressure, $P=3.45$ bar

From Fig. 10, the average motor pressure decreases from 2.379 to 1.814, 2.053, and 2.322 bar by changing the flow mode from continuous to pulsating air flow of frequencies 1.5, 3, and 4.5 Hz, respectively.

As shown in Fig. 11, at main source pressure, $P=3.45$ bar, the average motor speeds are 312, 143.05, 225.4, and 289.8 r.p.m at continuous flow mode, $f=1.5$, 3, and 4.5 Hz, respectively. The results showed the same behavior for the motor torque and speed.

4.3 Pulsating flow at main source pressure, $P=5.17$ bar

From Fig. 12, the average motor pressure decreases from 2.83 to 2.11, 2.38, and 2.85 bar by changing the flow mode from continuous to pulsating air flow of frequencies 1.5, 3, and 4.5 Hz, respectively.

As shown in Fig. 13, at main source pressure, $P=5.17$ bar, the average motor speeds are 371, 161.82, 267.1, and 361.97 r.p.m at continuous flow mode, $f=1.5$, 3, and 4.5 Hz, respectively. The results showed the same behavior for the motor torque and speed.

5 Data collection and comparison of simulation output

A comparison of simulation results at different pressures and frequencies is presented in Table 1. It lists the values of the direct effect of the main source pressure and pulse flow frequency on the pneumatic motor speed, average motor pressure, and motor torque calculated by Eq. (2) for a motor displacement of 100 cm^3/rev and assuming 100% motor

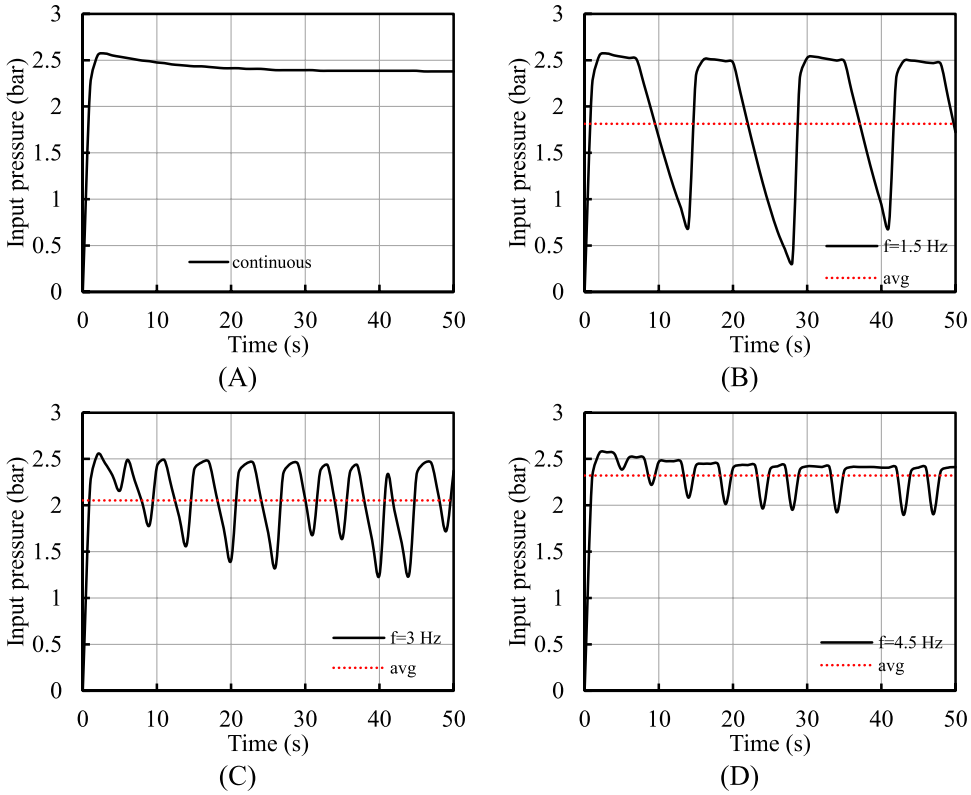

Fig. 10 Pneumatic motor pressure: **A** continuous, **B** $f=1.5$ Hz, **C** $f=3$ Hz, and **D** $f=4.5$ Hz at main source pressure, $P=3.45$ bar

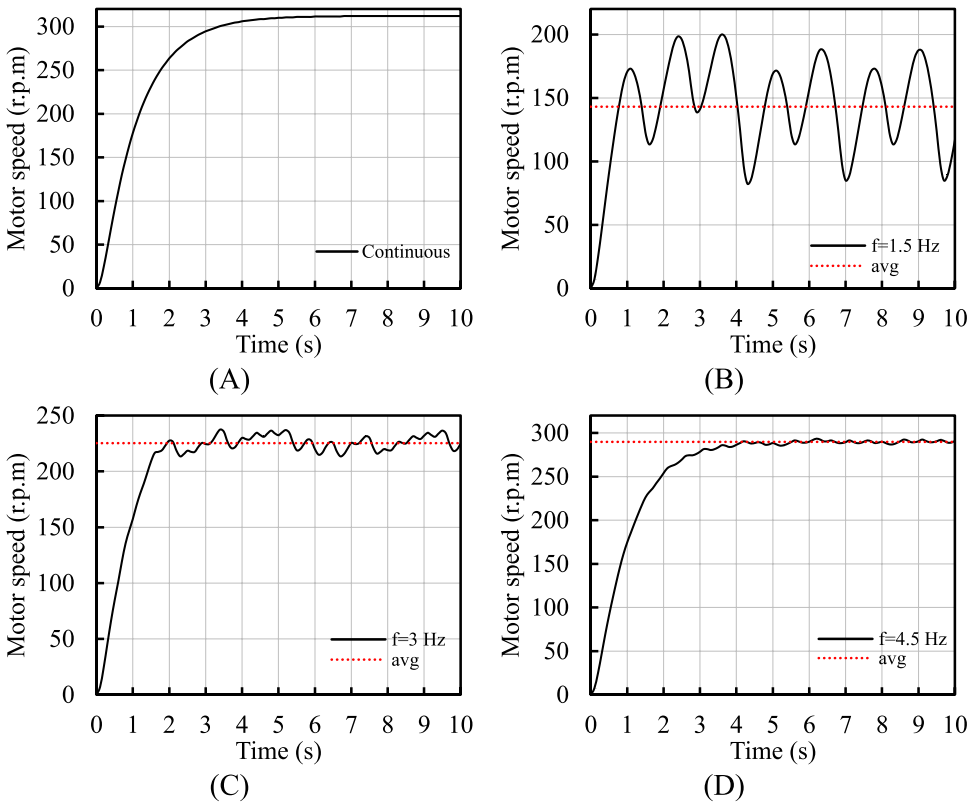

Fig. 11 Motor speed versus time at **A** continuous, **B** $f=1.5$ Hz, **C** $f=3$ Hz, and **D** $f=4.5$ Hz at main source pressure, $P=3.45$ bar

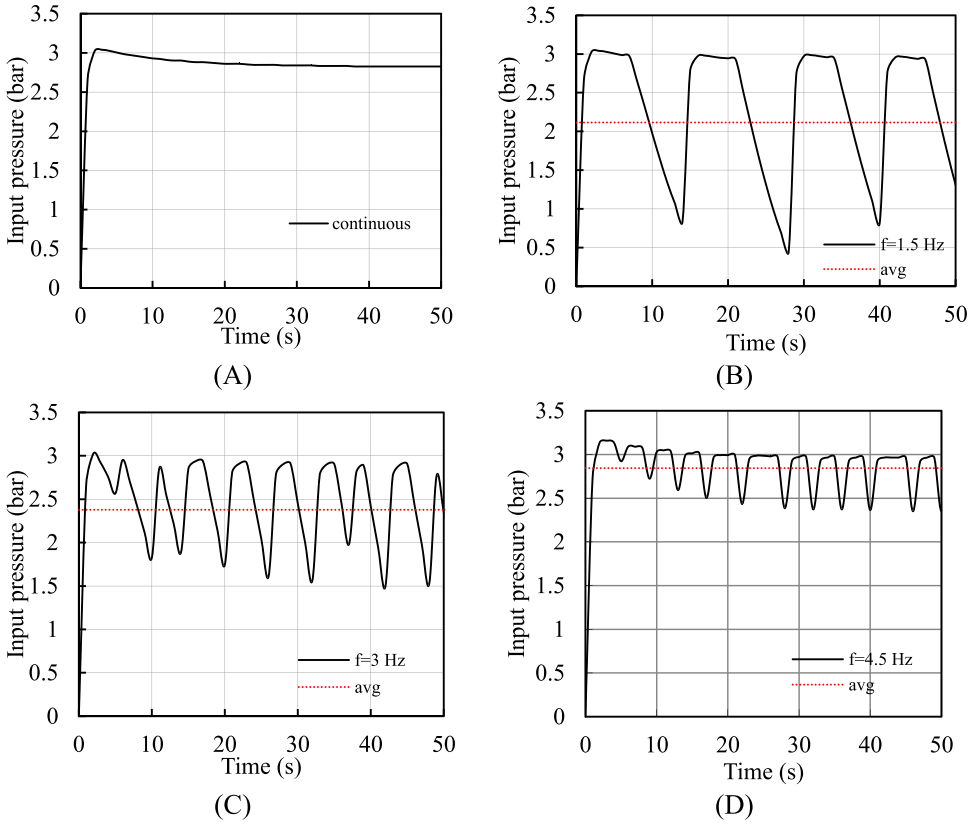

Fig. 12 Pneumatic motor pressure: **A** continuous, **B** $f=5$ Hz, **C** $f=3$ Hz, and **D** $f=1$ Hz at main source pressure, $P=5.17$ bar

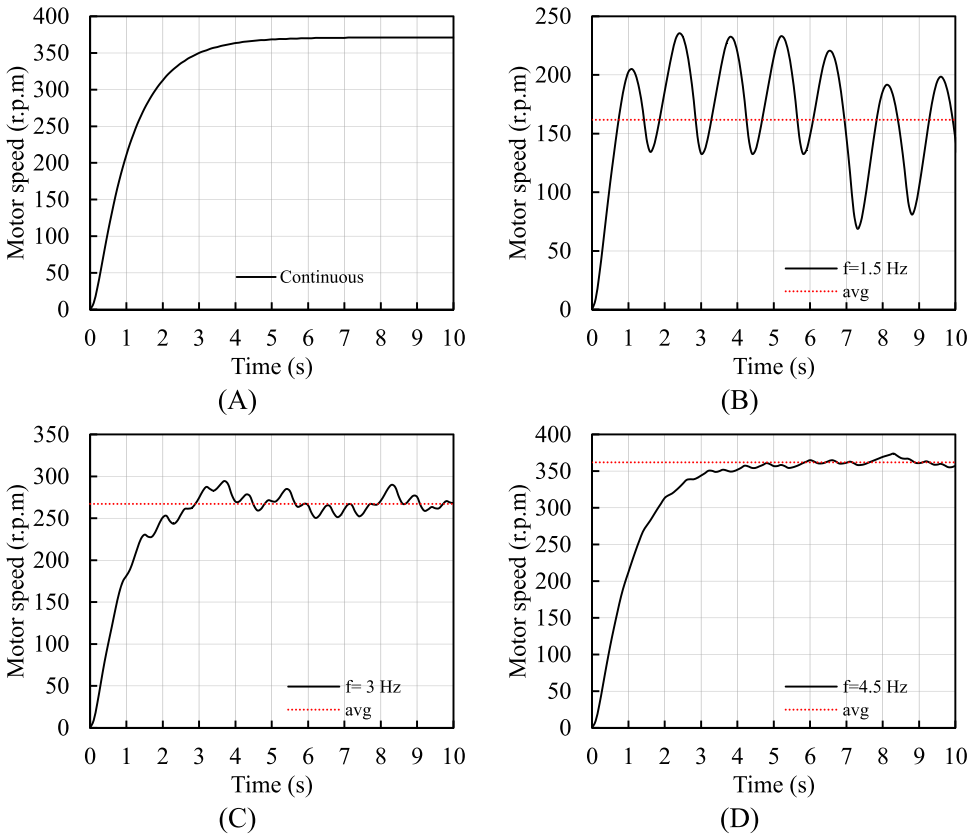

Fig. 13 Motor speed versus time at **A** continuous, **B** $f=5$ Hz, **C** $f=3$ Hz, and **D** $f=1$ Hz at main source pressure, $P=5.17$ bar

efficiency. It also shows the strong influence of the pulse flow frequency on motor performance. For example, at an inlet pressure of 1.72 bar with a frequency of 1.5 Hz, the motor speed and pressure were reduced by 52% and 22.7%, respectively. The same conclusion at different inlet pressures can be inferred. This confirms the presented research's idea of using compressed air's pulse flow in pneumatic systems to control the pneumatic motor's speed and torque.

Figure 14 shows the effect of mode change from continuous to pulsating flow with different frequencies and main source pressures on the motor pressure, torque, and speed. For example, at an inlet pressure of 1.72 bar with a frequency of 1.5 Hz, the motor inlet pressure, torque, and speed were reduced by 22.68%, 22.89%, and 51.51%, respectively. The same conclusion at different inlet pressures can be inferred. This confirms the validity of the proposed idea of using the pulse flow of compressed air in pneumatic systems to control the inlet pressure, torque, and speed of the pneumatic motor.

The pressure and flow rate values describe the fluid power, and by changing the source pressure value, the flow rate also changes. For example, Fig. 14A shows that changing the source pressure value from 1.72 to 3.45 to 5.17 bar increases the motor's input pressure. This is reflected in the motor's torque, as shown in Fig. 14B. At continuous flow represented by 0 Hz (normally opened), with increasing source pressure from 1.72 to 3.45 to 5.17 bar, the torque increased from 2.49 to 3.78 to 4.50 N.m. It is worth noting here that there is no linear relationship between the increase in the source pressure and the accompanying increase in the motor torque. Instead, the relationship is more like a polytropic, where the torque increment with pressure changing from 1.72 to 3.45 bar was below 1.29 N.m. In comparison, this change decreased to less than 0.72 N.m, with the pressure increasing from 3.45 to 5.17 bar.

The pressure and flow rate values describe the fluid power, and by changing the source pressure value, the flow rate also changes. For example, Fig. 10A shows that changing the source pressure value from 1.72 to 3.45 to 5.17 bar increases the motor's inside pressure. This is reflected in the motor's torque, as shown in Fig. 10B. At continuous flow represented by 0 Hz (normally opened), the torque increased from 2.49 to 3.78 to 4.50 N.m. It is worth noting here that there is no linear relationship between increasing source pressure and the accompanying increase in the motor torque. Instead, the relationship is more like a polytropic, where the torque increment with pressure changing from 1.72 to 3.45 bar was below 1.29 N.m. In comparison, this change decreased to less than 0.72 N.m, with the pressure increasing from 3.45 to 5.17 bar.

On the other hand, with increasing source pressure, the motor speed increases, as shown in Fig. 10C. In addition to the source pressure effect, a great influence appears here, which is this research's core focus, the pulse flow frequency changes the pressure, motor torque, and motor speed for every source pressure. It implies that the source pressure and pulse flow frequency affect the motor speed and torque. Moreover, it gives the assurance that we can control the motor torque and speed through the pulse flow. For example, at continuous flow represented by 0 Hz (normally opened), the motor speed increased from 205 to 312 to 371 r.p.m. It is worth noting that there is a linear relationship between increasing source pressure and the accompanying motor speed. This explanation is derived from the graph. On the other hand, the motor speed increased from 161.82 to 267.10 to 361.97 r.p.m at 5.17 bar and frequencies of 1.5, 3, and 4.5 Hz, respectively. There is no linear relationship between increasing flow frequency and the accompanying motor speed. Instead, the relationship is more like a polytropic, with increased motor speed. This indicates that with increasing frequency, the compressibility effect decreases.

Table 1 Pneumatic motor average inlet pressure and speed versus applied pressure and frequency

Pressure (bar)	Frequency (Hz)	Pneumatic motor average pressure (bar)	Pneumatic motor average torque (N.m)	Pneumatic motor average speed (r.p.m)
1.72	0.0	1.565	2.49	205.00
	1.5	1.210	1.92	99.40
	3.0	1.350	2.15	148.80
	4.5	1.530	2.43	189.00
3.45	0.0	2.379	3.78	312.00
	1.5	1.814	2.89	143.05
	3.0	2.053	3.27	225.40
	4.5	2.322	3.70	289.80
5.17	0.0	2.830	4.50	371.00
	1.5	2.110	3.36	161.82
	3.0	2.380	3.79	267.10
	4.5	2.850	4.53	361.97

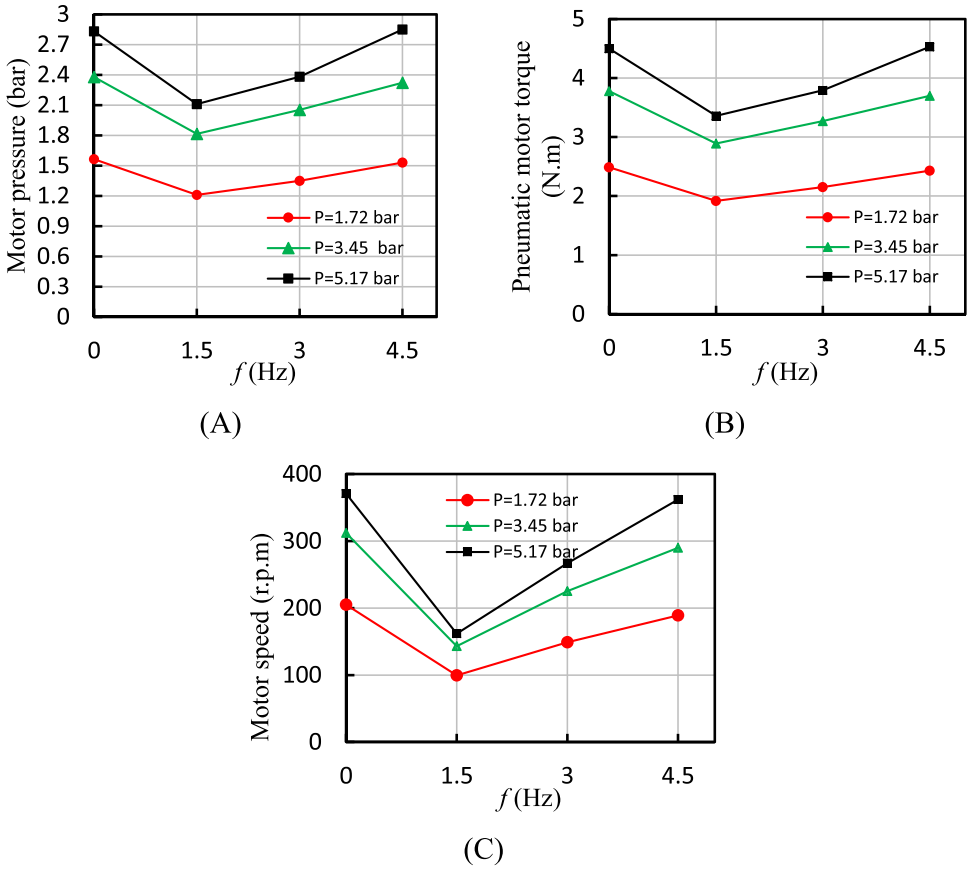

Fig. 14 Flow rate, cylinder rod linear speed, and cylinder force versus pressure and frequency

6 Mathematical correlation results

The motor torque and speed depend on the main source pressures (P) and frequencies (f). By the simulation results, the least-squares method is used to calculate the mathematical correlation coefficient [22, 24]. The fitted mathematical correlation is used in predicting the motor torque (T_{theo}) and speed (N) at any main source P and f for a wide range, expressed by:

$$N = (55.9624) \times P^{0.544} \times f^{0.6388} \tag{6}$$

$$T_{theo} = (1.3261) \times P^{0.5383} \times f^{0.2063} \tag{7}$$

Tables 2 and 3 show a comparison between the simulation results and mathematical correlation response for motor torque and speed, respectively.

Figures 15 and 16 show the predicted effect of pulsating air frequency and main source pressure on the motor torque and speed. The motor torque increases with increasing pulsating air frequency. In addition, the motor torque increases with increasing main source pressure. In contrast, the motor speed increases with increasing pulsating air frequency and main source pressure. The effect of frequency is strongly evident in both motor torque and speed.

7 Conclusions

From the results, the methods of controlling pneumatic motors in real life using proportional control valves, which is very complicated and expensive, can be replaced by the proposed pulse flow control. The effect of the pulsating air flow on the precise control of pneumatic motors is also evident and has the same function as the proportional control

Table 2 Comparison between the simulation results and mathematical correlation response for motor torque

P (bar)	f (Hz)	Simulation results, torque (N.m)	Mathematical correlation response (N.m)	Error (%)
1.72	1.5	1.92	1.93	−0.55
	3.0	2.15	2.22	−3.60
	4.5	2.43	2.42	0.33
3.45	1.5	2.89	2.80	2.83
	3.0	3.27	3.23	0.92
	4.5	3.70	3.52	4.79
5.17	1.5	3.36	3.49	−3.90
	3.0	3.79	4.02	−6.28
	4.5	4.53	4.37	3.32

Table 3 Comparison between the simulation results and mathematical correlation response for motor speed

P (bar)	f (Hz)	Simulation results, motor speed (r.p.m)	Mathematical correlation response (r.p.m)	Error (%)
1.72	1.5	99.40	97.38	2.02
	3.0	148.80	151.63	−1.91
	4.5	189.00	196.47	−3.95
3.45	1.5	143.05	142.21	0.59
	3.0	225.40	221.43	1.76
	4.5	289.80	286.90	1.00
5.17	1.5	161.82	177.21	−9.51
	3.0	267.10	275.93	−3.31
	4.5	361.97	357.51	1.23

valve. The rotational speed and torque of the pneumatic motor are controlled depending on the pulse flow frequency of air at any inlet source pressure. The pulse flow frequency of compressed air is synthesized, generated, and controlled by an electrical control circuit. The design and simulation for this purpose were done using the PLC technique. The pneumatic cylinder-air pressure and discharged air flow rate were measured using pressure and flow meter data loggers and validated with the simulation results. In the present work, Automation Studio is used to simulate the motor speed and pressure in a pneumatic motor. The conclusions from the study are summarized as follows:

(1) The pulsating air flow technique strongly controls the performance of pneumatic actuators with reasonable cost and setup facilities, unlike the other traditional systems.
(2) On the other hand, it provides the flexibility to convert the output using a controller to modify the fixed output actuators to work with a wide range of variable speed and torque, unlike the other traditional systems of fixed output.
(3) The software "Automation Studio" showed a realistic result, making it trustable for the preliminary design of the hydraulic and pneumatic system and simulation studies for different systems' behavior before building the circuit.
(4) An experimental implementation of a pulsating flow of compressed air on the speed and force of a pneumatic cylinder rod at a source pressure of 5.17 bar was made.
(5) The experimental results were used to validate the Automation Studio simulation results for the same conditions, and a close agreement in pneumatic cylinder performance was achieved.
(6) The pulse flow frequency of compressed air significantly affects the pneumatic motor performance through output motor torque and speed.
(7) As the pulsating flow frequency of compressed air decreased from 4.5, 3, and 1.5 Hz, the motor pressure and torque decreased.
(8) The frequency effect on the pneumatic motors' performance was simulated based on the motor speed and torque. The results showed a drop in the motor speed with decreasing frequency.
(9) The pulsating air flow technique can limit the actuator torque and speed to a required value to achieve the optimum working parameter depending on the frequency.
(10) An empirical correlation was developed to predict the T_{theo} and N at any main source P and f for a wide range, expressed by

$$N = 55.96 \times P^{0.544} \times f^{0.6388}$$
$$T_{theo} = 1.33 \times P^{0.5383} \times f^{0.2063}$$

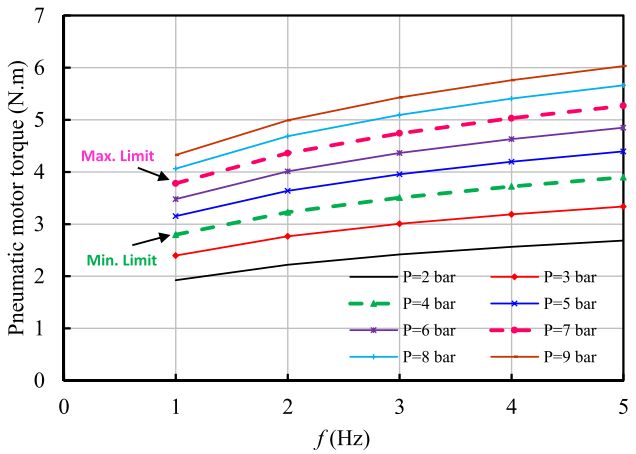

Fig. 15 Effect of pulsating air frequency on the motor torque at different main source pressures

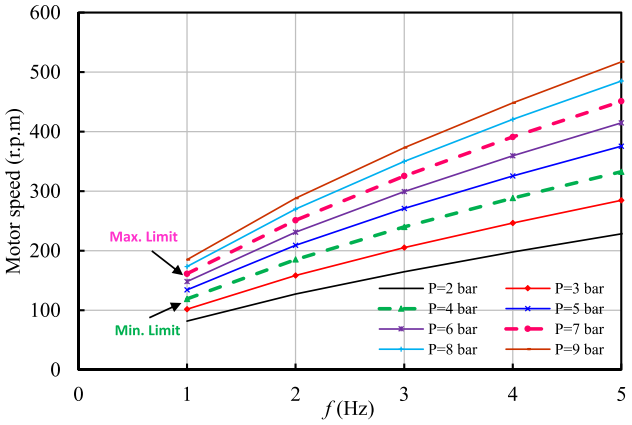

Fig. 16 Effect of pulsating air frequency on the motor speed at different main source pressures

Author contribution Mohamed A. Aziz: conceptualization, laboratory experiments, investigation, supervision, project administration, writing, the main search's idea. Ernesto Benini: methodology, investigation. Mohamed A. Khalifa: HMI software, visualization, validation. Osama A. Gaheen: laboratory experiments, investigation, data curation, writing, apparatus control design. Mostafa E. A. Elsayed rewrote and paraphrased the article, performed validation analysis, implemented HMI software, and revised the abstract and conclusion.

Funding Open access funding provided by Università degli Studi di Padova within the CRUI-CARE Agreement.

Declarations

Conflict of interest The authors declare no competing interests.

References

1. Soliman MA et al (2021) Modelling and implementation of soft bio-mimetic turtle using echo state network and soft pneumatic actuators. Sci Rep 11(1):1–11. https://doi.org/10.1038/s41598-021-91136-z
2. Xu H, Zhang L (2021) A software and hardware design scheme of intelligent valve positioner. E3S Web of Conferences. Vol. 268. EDP Sciences. https://doi.org/10.1051/e3sconf/202126801067
3. Oguntosin V, Nasuto SJ, Hayashi Y (2017) Embedded fuzzy logic controller for positive and negative pressure control in pneumatic soft robots. 2017 UKSim-AMSS 19th International Conference on Computer Modelling & Simulation (UKSim). IEEE. https://doi.org/10.1109/UKSim.2017.41
4. Blagojević V et al (2019) Automatic Generation of the PLC programs for the sequential control of pneumatic actuators. Facta Universitatis Ser: Mech Eng 17(3):405–414. https://doi.org/10.22190/FUME190123033B
5. Qi H, Bone GM, Zhang Y (2019) Position control of pneumatic actuators using three-mode discrete-valued model predictive control. Actuators. 8(3) Multidisciplinary Digital Publishing Institute. https://doi.org/10.3390/act8030056
6. Ali HI et al (2009) A review of pneumatic actuators (modeling and control). Aust J Basic Appl Sci 3(2):440–454
7. Lee HK, Choi GS, Choi GH (2002) A study on tracking position control of pneumatic actuators. Mechatronics 12(6):813–831. https://doi.org/10.1016/S0957-4158(01)00024-1
8. Andrikopoulos G, Nikolakopoulos G, Manesis S (2014) Advanced nonlinear PID-based antagonistic control for pneumatic muscle actuators. IEEE Trans Industr Electron 61(12):6926–6937. https://doi.org/10.1109/TIE.2014.2316255
9. Renn J-C, Liao C-M (2004) A study on the speed control performance of a servo-pneumatic motor and the application to pneumatic tools. Int J Adv Manuf Technol 23(7–8):572–576. https://doi.org/10.1007/s00170-003-1757-0
10 Chen Y et al (2017) Characterization and control of a pneumatic motor for MR-conditional robotic applications. IEEE/ASME Trans Mechatronics 22(6):2780–2789. https://doi.org/10.1109/TMECH.2017.2767906
11. Takemura F et al (2000) Control of a hybrid pneumatic/electric motor." Proceedings. 2000 IEEE/RSJ International Conference on Intelligent Robots and Systems (IROS 2000)(Cat. No. 00CH37113). Vol. 1. IEEE. https://doi.org/10.1109/IROS.2000.894606
12. Bone GM, Chen X (2012) Position control of hybrid pneumatic-electric actuators. In 2012 American Control Conference (ACC), pp. 1793–1799. IEEE. https://doi.org/10.1109/ACC.2012.6315400
13 Rouzbeh B et al (2019) Design, implementation and control of an improved hybrid pneumatic-electric actuator for robot arms. IEEE Access 7:14699–14713. https://doi.org/10.1109/ACCESS.2019.2891532
14 Stoianovici Dan et al (2007) A new type of motor: pneumatic step motor. IEEE/ASME Trans Mechatronics 12(1):98–106. https://doi.org/10.1109/TMECH.2006.886258
15. Chen S-Y, Gong S-S (2017) Speed tracking control of pneumatic motor servo systems using observation-based adaptive dynamic sliding-mode control. Mech Syst Signal Process 94:111–128. https://doi.org/10.1016/j.ymssp.2017.02.025
16 Xu Y et al (2021) Experimental investigation of pneumatic motor for transport application. Renew Energy. https://doi.org/10.1016/j.renene.2021.07.072
17. Xu Y et al (2021) Experimental study on small power generation energy storage device based on pneumatic motor and compressed air. Energy Conver Manag 234:113949. https://doi.org/10.1016/j.enconman.2021.113949
18. Dong Q, Liu X, Qi H, Zhou Y (2020) Vibro-acoustic prediction and evaluation of permanent magnet synchronous motors. Proc Inst Mech Eng Part D: J Automobile Eng 234(12):2783–2793. https://doi.org/10.1177/0954407020919659
19. Kan F, Liu X, Xin X, Jiejie Xu, Huang Hu, Wang Y (2018) Analysis and evaluation of the leakage failure for clutch sleeve and shell. Eng Fail Anal 88:1–12. https://doi.org/10.1016/j.engfailanal.2018.02.008
20. Nahal M, Khelif R (2021) A finite element model for estimating time-dependent reliability of a corroded pipeline elbow. Int J Struct Integr 12(2):306–321. https://doi.org/10.1108/IJSI-02-2020-0021
21. Yang Y-J, Wang G, Zhong Q, Zhang H, He J, Chen H (2021) Reliability analysis of gas pipeline with corrosion defect based on finite element method. Int J Struct Int 12(6):854–863. https://doi.org/10.1108/IJSI-11-2020-0112
22. Gaheen OA, Benini E, Khalifa MA, Aziz MA (2022) Pneumatic cylinder speed and force control using controlled pulsating flow. Eng Sci Technol Int J 35:101213. https://doi.org/10.1016/j.jestch.2022.101213
23. Gaheen OA, Benini E, Khalifa MA, El-Salamony ME, Aziz MA (2021) Experimental investigation on the convection heat transfer enhancement for heated cylinder using pulsated flow. Therm Sci Eng Progress 26:101055. https://doi.org/10.1016/j.tsep.2021.101055
24. Gaheen OA, Aziz MA, Hamza M, Kashkoush H, Khalifa MA (2022) Fluid and structure analysis of wind turbine blade with winglet. J Adv Res Fluid Mech Therm Sci 90(1):80–101. https://doi.org/10.37934/arfmts.90.1.80101